Ferromagnetic-Resonance Field and Linewidth in an Anisotropic Magnetic Metallic Medium

C. Vittoria and G. C. Bailey
Naval Research Laboratory, Washington, D. C. 20390

R. C. Barker* and A. Yelon*
Yale University, New Haven, Connecticut 06520
(Received 7 August 1972)

We have calculated the ferromagnetic-resonance (FMR) field and linewidth in an anisotropic metallic medium in contrast to previous calculations done by others for an isotropic medium or for polycrystalline materials. The Landau–Lifshitz equation of motion of the magnetization with an additional effective anisotropic field of cubic symmetry is coupled with Maxwell's equations. The solution yields a generalized secular equation which is quartic in k^2, where k is the propagation constant. We assume two limiting cases of the dynamic component of the magnetization $\vec{m}$ at the surface: (i) $\vec{m}$ is "free" to precess around the magnetic field $\vec{H}$ at the disk surface and (ii) $\vec{m}$ is totally constrained in precessing around $\vec{H}$. As an example, results are given for a (100) Ni disk and for $\vec{H}$ in the plane of the disk and at various angles with respect to the ⟨100⟩ axis. At 300 °K the FMR field (ω_σ/γ) is greater than its insulator value of 3072 Oe by 92 and 89 Oe, for H along the ⟨100⟩ and ⟨110⟩ axes, respectively; the linewidth is nearly isotropic and equal to 262 Oe. However, at 77 °K, where the anisotropy fields have a greater influence, the FMR fields are 341 and 207 Oe greater than the isotropic insulator value; the linewidth is anisotropic and equal to 660 and 424 Oe for the two respective directions. For the above cases, $\vec{m}$ is assumed to be pinned at the surface. The results which are also given for unpinned surface spins do not differ qualitatively. All the results have been obtained for two different frequencies, 9.4 and 24.0 GHz. Contrary to intuitive feelings, the anisotropy in the linewidth is inversely proportional to frequency. This is due to the fact that the anisotropy field becomes comparable to the resonant field as the frequency is lowered. We have thus found that, although exchange-conductivity effects are small at room temperature, they are quite significant in determining the resonance parameters at moderately low temperatures.

I. INTRODUCTION

One of the problems in the field of ferromagnetic resonance (FMR) is the separation of surface and volume preparation effects from effects characteristic of the pure material. This is particularly true for films where the ratio of surface area to volume is very large. During the past several years, improvements[1] have occurred in the production of metal samples, and in particular, very good thin single-crystal plates with few surface and volume defects have been produced. These plates represent almost an ideal means to connect the FMR-derived parameters to the material itself, independent of preparation effects.

Unfortunately, although the experimental means to achieve high-quality samples have advanced, the theory for metal films has lagged in explaining the FMR of metal single crystals. In general, the magnetic parameters, such as the g factor, the magnetization, and the magnetocrystalline anisotropy constants, are obtained by making a critical assumption in the theory which, as we shall show, is not necessarily true. It is generally assumed, even in an *anisotropic* medium, that the shift in the FMR field due to the exchange-conductivity[2–4] effect is isotropic and independent of the direction of the applied field with respect to some crystallographic axis.

In this paper we extend earlier work[4] on linewidth and resonance field in isotropic metal plates to the anisotropic case. By comparing our results with those for anisotropic insulating plates, we obtain the exchange-conductivity shift as a function of angle. We find that this shift is anisotropic especially at low temperatures, when the conductivity and the magnetocrystalline anisotropy are both large.

The formalism involved in the calculations is developed in Sec. II. We assume that the sample is a semi-infinite plate and that the magnetization is uniform throughout the sample. The Landau–Lifshitz equation of motion for the magnetization is coupled with Maxwell's equations to obtain a secular equation for their simultaneous solution. We show that this equation reduces to previously well-known forms in simple limiting cases. From this equation, one obtains the values of the electromagnetic propagation vectors.

The surface impedance Z is introduced as in previous calculations[2,3] to reduce the number of variables required to specify the problem at the sample surface. The rf electric field is eliminated as a variable through the definition of Z. In contrast to the previous use of an isotropic[2–4] surface impedance, we assume an anisotropic surface im-

pedance to account for an anisotropic internal field $\vec{H}_0$ needed for resonance. Z is calculated for a given angle of $\vec{H}_0$ with respect to some crystallographic axis. The FMR field and linewidth, ω/γ and $\Delta\omega/\gamma$, are obtained from the real part of Z.

Although the calculations are applicable to any cubic magnetically anisotropic material, they are applied to the specific case of a thin disk of nickel in Sec. III. Nickel is chosen because it has large anisotropy constants, K_1 and K_2, particularly at low temperatures, because it has been studied extensively[5-8] by FMR, and hence the exchange constant A and the Landau–Lifshitz damping parameter are reasonably well known, and, finally, because high-quality thin single crystals can be grown in platelet form. We have obtained ω/γ and $\Delta\omega/\gamma$ for temperatures of 300 and 77 °K. At low temperatures one expects a large effect because the conductivity is large and the skin depth is small. Thus, the change with depth of the rf component of the magnetization is large and the induced exchange fields should be large. Furthermore, the anisotropy is also large. For convenience, we choose the thickness of the nickel sample to be 1 μm, larger than the skin depth. At temperatures below ~77 °K, the skin depth becomes anomalous and our present calculations would be inapplicable.

We also obtain results at two different frequencies (9.4 and 24.0 GHz) and for a variety of values for the conductivity σ, since this parameter may vary in actual samples as a result of a variation in purity from sample to sample.

II. THEORETICAL FORMULATION

A. Secular Equation

It has been shown over the years that the Landau–Lifshitz[4-7,9,10] and Gilbert forms[11] of the equation of motion can adequately describe the time dependence of the magnetization in magnetic metals. Since at temperatures well below the Curie temperature, both models give similar results, we will use the Landau–Lifshitz damping form for convenience:

$$\frac{1}{\gamma}\frac{d\vec{M}}{dt} = \vec{M}x(\vec{H}_0 + \vec{h} + \vec{h}_A + \vec{h}_{ex} + \vec{h}_\lambda) \ . \qquad (1)$$

The various terms in the parentheses, which are discussed in detail below, represent different effective magnetic fields acting upon the magnetization. Respectively, these terms are the static effective internal field, the rf Maxwellian field, the rf anisotropy field, the exchange field, and the effective damping field.

The static internal field $\vec{H}_0$ can be expressed in terms of the external field $\vec{H}_a$, the demagnetizing field $\vec{H}_d$, and the static cubic anisotropy field $\vec{H}_A$:

$$\vec{H}_0 = \vec{H}_a + \vec{H}_d + \vec{H}_A \ .$$

The explicit functional dependence of $\vec{H}_0$ on angle can be derived from

$$\vec{H}_0 = -\vec{\nabla}_\alpha F/M_0 \ , \qquad (2)$$

where $M_0 = |\vec{M}|$. The gradient operator $\vec{\nabla}_\alpha$ is defined with respect to the direction cosines measured from the crystal axes. F is the magnetic free energy:

$$F = -\vec{H}_a \cdot \vec{M} + 2\pi M_0^2 \alpha_2^2 + K_1(\alpha_1^2\alpha_2^2 + \alpha_1^2\alpha_3^2 + \alpha_2^2\alpha_3^2) + K_2(\alpha_1\alpha_2\alpha_3)^2 \ . \qquad (3)$$

In Eq. (3), the α's are the directional cosines of $\vec{M}$ with respect to the cubic ⟨100⟩ axes. K_1 and K_2 are the first- and second-order anisotropy constants, respectively. The first term on the right-hand side represents the Zeeman energy, the second the demagnetizing energy, and the third and fourth the magnetocrystalline anisotropy energies.

The form of the second term in Eq. (3), the demagnetizing energy, is dictated by our having taken the 2 (or y) axis to be a ⟨100⟩ axis normal to the plane of the plate as shown in Fig. 1. Further, we assume that, in the static situation, the magnetization is saturated, and that the sample is infinite in the x and z directions, so that the demagnetizing factor is 4π. This last assumption is reasonably good for plates with aspect ratios as low as 25.

Substituting Eq. (3) into (2), we get

$$\vec{H}_0 = \vec{H}_a - 4\pi M_0 \alpha_2 \vec{a}_y - 2K_1[\alpha_1(\alpha_2^2 + \alpha_3^2)\vec{a}_x + \alpha_2(\alpha_1^2 + \alpha_3^2)\vec{a}_y + \alpha_3(\alpha_1^2 + \alpha_2^2)\vec{a}_z]/M_0 - 2K_2(\alpha_1\alpha_2^2\alpha_3^2\,\vec{a}_x + \alpha_2\alpha_1^2\alpha_3^2\,\vec{a}_y + \alpha_3\alpha_1^2\alpha_2^2\,\vec{a}_z)/M_0 \ , \qquad (4)$$

where the a's are unit vectors. The second term in Eq. (4) is $\vec{H}_d$ and the third and fourth terms are $\vec{H}_A$.

The rf Maxwellian field $\vec{h}$, which is made up of

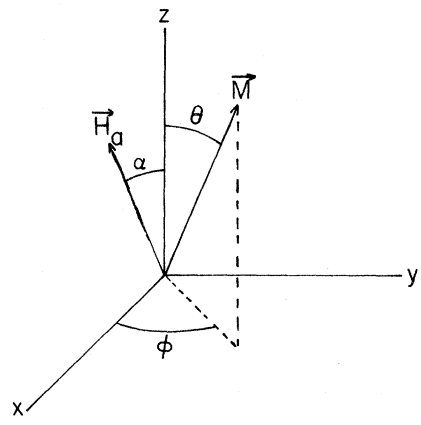

FIG. 1. Geometrical configuration of the applied field and the magnetization.

the incident, transmitted, reflected, and demagnetizing rf components, is not known *a priori*. Its value is determined by satisfying Maxwell's equations and the boundary conditions appropriate to these equations. These are discussed below.

The rf anisotropy field $\vec{h}_A$ is simply calculated by taking virtual variations of $\vec{H}_A$,[12]

$$\vec{h}_A = \delta\vec{H}_A \ . \tag{5}$$

Thus, for the three components of $\vec{h}_A$, we find

$$h_{Ax} = -(C_1 m_x + C_2 m_y + C_3 m_z)/M_0 \ , \tag{6a}$$

$$h_{Ay} = -(C_4 m_x + C_5 m_y + C_6 m_z)/M_0 \ , \tag{6b}$$

$$h_{Az} = -(C_7 m_x + C_8 m_y + C_9 m_z)/M_0 \ , \tag{6c}$$

where

$$C_1 = (2K_1/M_0)(1-\alpha_1^2) + (2K_2/M_0)\alpha_2^2\alpha_3^2 \ ,$$

$$C_2 = C_4 = 2\alpha_1\alpha_2[2K_1/M_0 + (2K_2/M_0)\alpha_3^2] \ ,$$

$$C_3 = C_7 = 2\alpha_1\alpha_3[2K_1/M_0 + (2K_2/M_0)\alpha_2^2] \ ,$$

$$C_5 = (2K_1/M_0)(1-\alpha_2^2) + (2K_2/M_0)\alpha_1^2\alpha_3^2 \ ,$$

$$C_6 = C_8 = 2\alpha_2\alpha_3[2K_1/M_0 + (2K_2/M_0)\alpha_1^2] \ ,$$

$$C_9 = (2K_1/M_0)(1-\alpha_3^2) + (2K_2/M_0)\alpha_1^2\alpha_2^2 \ .$$

Each term $h_{A\beta}$ represents the rf component of $\vec{h}_A$ in the β direction. The rf field $\vec{h}_A$ is present only if there is a small deviation of $\vec{M}$ from its equilibrium position $\vec{M}_0$.

The effective exchange field $\vec{h}_{ex}$ is obtained from

$$\vec{h}_{ex} = (2A/M_0^2)\nabla^2\vec{M} \ ,$$

where A is the exchange stiffness constant. In a metal, the attenuation of the rf field generates a spatial variation of $\vec{M}$, and results in $\vec{h}_{ex}$.

The Landau–Lifshitz (LL) damping field $\vec{h}_\lambda$ has the form

$$\vec{h}_\lambda = -(\lambda/\gamma M_0^2)\,\vec{M}\times(\vec{H}_0 + \vec{h} + \vec{h}_A) \ ,$$

where λ is the LL phenomenological damping term, assumed to be isotropic.[13] The form of $\vec{h}_\lambda$ is such that the magnitude of $\vec{M}$ is conserved. In principle, $\vec{h}_{ex}$ should be included in this term, along with $\vec{H}_0$, $\vec{h}$, and $\vec{h}_A$. However, the effect of including $\vec{h}_{ex}$ is so small,[14] and the mathematical complication so great, that we neglect it here.

Equation (1) must be solved simultaneously with Maxwell's equations. In Gaussian units

$$\vec{\nabla}\times\vec{E} = -\frac{1}{c}\frac{\partial}{\partial t}(\vec{H} + 4\pi\vec{M}) \ , \tag{7a}$$

$$\vec{\nabla}\times\vec{H} = \frac{4\pi\sigma}{c}\vec{E} \ , \tag{7b}$$

$$\vec{\nabla}\cdot(\vec{H} + 4\pi\vec{M}) = 0 \ . \tag{7c}$$

The Maxwellian field $\vec{H}$ which appears in Eqs. (7) is composed of two terms

$$\vec{H} = \vec{H}_0 + \vec{h} \ . \tag{8a}$$

The internal fields $\vec{E}$ and $\vec{H}$ are subject to the usual electromagnetic boundary conditions at the surfaces of the plate.

The magnetization $\vec{M}$ can likewise be decomposed into static and rf components:

$$\vec{M} = \vec{M}_0 + \vec{m} \ , \tag{8b}$$

where $\vec{M}_0$ is parallel to $\vec{H}_0$. In this paper we shall consider two limiting boundary conditions on the dynamic magnetization $\vec{m}$: (i) $\vec{m}=0$ at the surface (usually referred to as the full-pinning condition[15]) and (ii) $\partial\vec{m}/\partial y = 0$ at the surface (the free-pinning condition). In practice, any condition between these two extremes is possible.[10]

Equation (1) and the set of Eqs. (7) are coupled through the magnetization $\vec{M}$. In the microwave-frequency range, the displacement-current term that would appear in Eq. (7b) is neglected since it is small compared with the conduction-current term. There are nine variables ($\vec{M}$, $\vec{E}$, and $\vec{H}$) in Eq. (1) and the set of Eqs. (7).

In an FMR experiment the external rf magnetic field is small so that the deviation of $\vec{M}$ from its equilibrium direction $\vec{M}_0$ is small, i.e.,

$$|\vec{h}| \ll |\vec{H}_0| \quad \text{and} \quad |\vec{m}| \ll |\vec{M}_0| \ .$$

Wave propagation in the sample is assumed in the y direction, since the sample is symmetrically excited by external linear polarized waves traveling in the $\pm y$ direction. That is, $\vec{m}$ and $\vec{h}$ are both proportional to $e^{ky-j\omega t}$. Of course, for finite-size samples, propagation in the x and z directions inside the medium must be considered.[16,17] Magnetostatic-mode excitations[18] in films may arise when this is the case. But for a semi-finite film, these modes are not excited.

The variable $\vec{E}$ in the set of Eqs. (7) can be eliminated by combining Eqs. (7a) and (7b):

$$\vec{\nabla}\times(\vec{\nabla}\times\vec{H}) = -\frac{4\pi\sigma}{c^2}\frac{\partial}{\partial t}(\vec{H} + 4\pi\vec{M}) \ . \tag{9}$$

Substituting Eqs. (8a) and (8b) into (9), we get

$$k^2 h_y \vec{a}_y - k^2\vec{h} = -j\frac{4\pi\sigma\omega}{c^2}(\vec{h} + 4\pi\vec{m}) \ . \tag{10}$$

Equation (10) may be written in component form:

$$m_x + Qh_x = 0 \ , \tag{11a}$$

$$4\pi m_y + h_y = 0 \ , \tag{11b}$$

$$m_z + Qh_z = 0 \ , \tag{11c}$$

where $Q = (1/4\pi)(1 + \frac{1}{2}j\delta_0^2 k^2)$ and $\delta_0^2 = c^2/2\pi\sigma\omega$. Equation (11b) corresponds to the Kittel rf demagnetizing field, which is introduced directly into the equations of motion via Eq. (4) as a separate field component by most authors.[19] It enters automatically through the use of Maxwell's equa-

tions. Obviously, the dc demagnetizing field is not contained in Eq. (11b) but is found in Eq. (4).

Substituting Eqs. (8a) and (8b) into (1), and neglecting nonlinear terms in $\vec{m}$ and $\vec{h}$, yields

$$\left(\frac{j\omega}{\gamma}+\frac{\lambda}{\gamma}\frac{H_0}{M_0}\right)\vec{m}=\vec{M}_0\times\vec{m}\left(\frac{2A}{M_0}k^2-H_0\right)$$
$$+\vec{M}_0\times(\vec{h}+\vec{h}_A)+\frac{\lambda}{\gamma}(\vec{h}+\vec{h}_A)-\frac{\lambda}{\gamma}[\vec{U}\cdot(\vec{h}+\vec{h}_A)]\vec{U}\ , \tag{12}$$

where

$$\vec{U}=\alpha_1\vec{a}_x+\alpha_2\vec{a}_y+\alpha_3\vec{a}_z\ . \tag{13}$$

The variable $\vec{h}$ is eliminated from (12) by relating $\vec{m}$ to $\vec{h}$ through Eqs. (11). Substituting Eqs. (6) into Eq. (12), we obtain a set of three equations in terms of m_x, m_y, and m_z. The three equations are of the form

$$[A]\cdot\vec{m}=0\ , \tag{14}$$

where $[A]$ is a 3×3 matrix whose elements are given by

$$[A]=\begin{bmatrix} a_{11}+c_{11} & a_{12}+c_{12} & a_{13}+c_{13} \\ a_{21}+c_{21} & a_{22}+c_{22} & a_{23}+c_{23} \\ a_{31}+c_{31} & a_{32}+c_{32} & a_{33}+c_{33} \end{bmatrix}\ .$$

The a's are the matrix elements of $[A]$ if $K_1=K_2=0$ (no magnetic anisotropy). In the Appendix, the a_{ij} and c_{ij} are defined in terms of K_1, K_2, M_0, H_0, λ, γ, σ, and A.

Now, as we have pointed out above, the form of the LL damping term is such that the magnitude of $\vec{M}$ is conserved. In the linear approximation (neglecting nonlinear terms of the form $m_\alpha m_\beta$, $h_\alpha h_\beta$, and $m_\alpha h_\beta$, where α and β mean x, y, or z, taken cyclically) this means that $\vec{m}$ is perpendicular to $\vec{M}_0$. For example, it is easy to show that for $\vec{M}_0$ in the film plane

$$m_z=-m_x\tan\theta\ , \tag{15}$$

where θ is the angle between $\vec{M}_0$ and the z axis (see Fig. 1). In general, the three equations in Eq. (14) are not linearly independent. Thus, we may reduce the 3×3 matrix to a 2×2 matrix $[A']$.

There exist nontrivial solutions for $\vec{m}$ if

$$\det[A']=0\ . \tag{16}$$

This results in a secular equation which is quartic in k^2:

$$(a^2+b^2+2\Omega a)\alpha_2^2+(1-\alpha_2^2)[ad+bc+\Omega(a+d)]+\Omega^2$$
$$+[(c_{11}c_{22}+c_{11}c_{33}+c_{22}c_{33})-(c_{31}c_{13}+c_{21}c_{12}+c_{23}c_{32})]$$
$$-(a_{31}c_{13}+a_{13}c_{31}+a_{32}c_{23}+a_{23}c_{32}+a_{21}c_{12}+a_{12}c_{21})$$
$$-[d(1-\alpha_2^2)(c_{11}+c_{33})+a(1-\alpha_1^2)c_{33}+a(1-\alpha_3^2)c_{11}$$
$$+a(2-\alpha_1^2-\alpha_3^2)c_{22}]-\Omega(c_{11}+c_{22}+c_{33})=0\ . \tag{17}$$

The definitions of a, b, c, d, and Ω are given in the Appendix. Had we taken the determinant of $[A]$, we could have obtained the same dispersion relation, plus the additional unphysical root $\omega/\gamma=0$.

By considering various limiting cases of Eq. (17), we can show that previously derived secular equations are contained in it. Several such cases are treated below.

1. Isotropic Metals

We recall that all of the c's are zero if $K_1=K_2=0$, in which case Eq. (17) reduces to

$$(a^2+b^2+2\Omega a)\alpha_2^2+(1-\alpha_2^2)$$
$$\times[ad+bc+\Omega(a+d)]+\Omega^2=0. \tag{18}$$

The secular equation given in Eq. (18) is exactly the same as the one obtained previously for isotropic magnetic metal plates[4] and is applicable for an arbitrary direction of $\vec{M}_0$ (*in or out* of the film plane). Equation (18) is quartic in k^2, giving four pairs of roots, where the members of a given pair are negatives of each other. Furthermore, with $\vec{M}_0$ *in* the plane of the film ($\alpha_2=0$), Eq. (18) becomes (after multiplying by Q^2)

$$Q\{[a'd+b'c+\Omega(a'+d')]+Q\Omega^2\}=0\ ,$$

where

$$a'=Qa\ ,\quad b'=Qb,\quad d'=Qd. \tag{19a}$$

Now, $Q=0$ is the nonmagnetic solution which results in the classical skin depth. The quantity inside the brackets is a cubic equation in k^2 which was derived by Ament and Rado.[2] Finally, with $\vec{M}_0$ perpendicular to the film plane ($\alpha_2=1$), Eq. (18) becomes

$$a^2+b^2+2\Omega a+\Omega^2=0\ . \tag{19b}$$

The roots of k^2 can be easily solved from Eq. (19b) to give the dispersion relation

$$\Omega=-a\pm jb\ .$$

The form of the secular equation in Eq. (19b) was derived by Akhiezer[3] for perpendicular resonance.

2. Anisotropic Insulators

For an insulating material the conductivity σ is 0 and the skin depth δ_0 is infinite. For unpinned boundary conditions, since there is no attenuation, only the $k=0$ mode will be excited. With no magnetic damping ($\lambda=0$) and with $A=0$, Eq. (17) then reduces to a very simple expression for the frequency of the FMR uniform-precession mode. Let us consider three special directions.

If $\vec{M}_0$ is perpendicular to the plane of the sample, but along the [010] axis, $\alpha_1=\alpha_3=0$ and $\alpha_2=1$. Equation (17) then yields

$$\omega/\gamma=H_0+2K_1/M_0\ .$$

Using Eq. (4), we obtain

$$H_0 = H_a - 4\pi M_0 .$$

Therefore,

$$\omega/\gamma = H_a - 4\pi M_0 + 2K_1/M_0 . \quad (20)$$

This is a well-known result.[19,20]

If $\vec{M}_0$ is in the film plane, along the [001] axis, $\alpha_1 = \alpha_2 = 0$ and $\alpha_3 = 1$. From Eq. (4), $H_0 = H_a$. Then from Eq. (17)

$$\frac{\omega}{\gamma} = \left[\left(H_a + \frac{2K_1}{M_0}\right)\left(H_a + \frac{2K_1}{M_0} + 4\pi M_0\right)\right]^{1/2} \quad (21)$$

If $\vec{M}_0$ is in the film plane, along the [101] axis, $\alpha_1 = \alpha_3 = 1/\sqrt{2}$ and $\alpha_2 = 0$. Equation (17) yields

$$\frac{\omega}{\gamma} = \left[\left(H_0 - \frac{K_1}{M_0}\right)\left(H_0 + \frac{2K_1}{M_0} + \frac{K_1}{2M_0} + 4\pi M_0\right)\right]^{1/2} .$$

From Eq. (4), we have

$$H_0 = H_a - K_1/M_0 ,$$

which gives

$$\frac{\omega}{\gamma} = \left[\left(H_a - \frac{2K_1}{M_0}\right)\left(H_a + \frac{K_1}{M_0} + \frac{K_2}{2M_0} + 4\pi M_0\right)\right]^{1/2} . \quad (22)$$

Thus, by taking some appropriate limits of Eq. (17), we have shown that some recognizable results can be generated.

3. *Anisotropic Metals*

We now consider the most general form of Eq. (17), including effects of exchange ($A > 0$), conductivity ($\sigma > 0$), magnetic damping ($\lambda > 0$), and anisotropy effects (K_1 and K_2 different from 0). However, we will restrict $\vec{M}_0$ to lie in the film plane, the (010) plane. In this case the secular equation [Eq. (17)] gives rise to a solution $Q = 0$ and a cubic equation in k^2:

$$\begin{aligned}[a'd + b'c + \Omega(a' + d')] + Q\Omega^2 \\ + Q[(c_{11}c_{22} + c_{11}c_{33} + c_{22}c_{33}) \\ - (c_{31}c_{13} + c_{21}c_{12} + c_{23}c_{32})] \\ - Q(a_{31}c_{13} + a_{13}c_{31} + a_{32}c_{23} \\ + a_{23}c_{32} + a_{21}c_{12} + a_{12}c_{21}) \\ - [d'(c_{11} + c_{33}) + a'(1 - \alpha_1^2)c_{33} \\ + a'(1 - \alpha_3^2)c_{11} + a'c_{22}] = 0 . \quad (23)\end{aligned}$$

As expected, the inclusion of anisotropy fields does not modify the "pure" nonmagnetic skin-depth mode $Q = 0$ discussed previously for the case of $K_1 = K_2 = 0$. However, since we are interested in the magnetic solution of the problem, we must solve the cubic equation. Although there are analytical ways[21] of solving for the roots, Eq. (23) is so cumbersome that an analytic solution becomes quite involved. We have solved the cubic equation numerically, by computer, and we will present a comprehensive study of the roots in another paper.

In Sec. IIB, we outline the method and obtain an expression for the surface impedance Z in terms of the roots of Eq. (23).

B. Surface Impedance

If we substitute one of the six k values (three pairs, positive and negative) obtained from Eq. (23) into Eq. (14), we obtain an internal magnetic rf field solution. As in the case of the isotropic metal,[2] each of these solutions corresponds to a linearly polarized wave. The total internal rf field is a linear combination of these eigenmode field solutions. The proper combination is determined uniquely by the boundary conditions. All solutions must satisfy the continuity of the rf electric and magnetic fields across the surfaces. In addition to this, we must specify a boundary condition on the magnetization. Here we assume one of the usual limiting cases: Either $\vec{m}$ is fully pinned at the surface ($\vec{m} = 0$) or it is completely unpinned ($\partial\vec{m}/\partial y = 0$). For what follows, we will assume that the rf excitation is applied symmetrically to the two surfaces of the sample, so that the internal rf field solutions are a symmetric function of y. In this case, the complete solution must be a sum of three hyperbolic cosines generated from each of the pairs of solutions with wave vector k_n, $n = 1$, 2, and 3.

Before writing and solving the equations which represent the boundary conditions, we introduce some transformed variables, in order to simplify the mathematics, and the surface impedance Z, in order to eliminate the rf electric field. For in-plane FMR, it is convenient to introduce a pair of transverse fields, h_t, and m_t, in the plane of the film and normal to $\vec{M}_0$. Thus,

$$m_x = \alpha_3 m_t , \quad m_z = -\alpha_1 m_t . \quad (24)$$

Each solution corresponding to a particular k_n must satisfy Maxwell's equations, and Eqs. (11) and (14), obtained from the equation of motion. From Eqs. (11)

$$m_t(n) = -Q_n h_t(n) , \quad (25)$$

where Q_n is the value of Q corresponding to k_n. Then, from Eqs. (14) and (25) it is relatively simple to show that

$$m_y(n) = v_n h_t(n) , \quad (26)$$

where

$$v_n = Q_n(b_n + \alpha_1 c_{23} - \alpha_3 c_{21})/(d + \Omega - c_{22}) . \quad (27)$$

In Eq. (27), b_n is the value of b (see the Appendix) corresponding to k_n.

In general, the surface impedance Z is a tensor property.[22] But for the characteristic polarizations of the system, reflected without change of polarization, it is a scalar[4] defined as

$$Z = (c/4\pi\sigma)\, e_t/h_t \ . \tag{28}$$

Using Eqs. (25)–(28), we may write the boundary-condition equations explicitly. For the case of completely free surface pinning

$$\sum_{n=1}^{3} X_n \cosh(k_n\, d/2) = h_0 \quad (\vec{h} \text{ continuous}) \ , \tag{29}$$

$$\sum_{n=1}^{3} X_n\, k_n \sinh(k_n\, d/2) = Z \quad (\vec{e} \text{ continuous}), \tag{30}$$

$$\sum_{n=1}^{3} X_n\, k_n\, Q_n \sinh(k_n\, d/2) = 0 \left(\frac{\partial m_t}{\partial y} = 0\right) \ , \tag{31}$$

$$\sum_{n=1}^{3} X_n\, v_n\, k_n \sinh(k_n\, d/2) = 0 \left(\frac{\partial m_y}{\partial y} = 0\right) \ . \tag{32}$$

For full pinning, Eqs. (31) and (32) become

$$\sum_{n=1}^{3} X_n\, Q_n \cosh(k_n\, d/2) = 0 \quad (m_t = 0) \ , \tag{31'}$$

$$\sum_{n=1}^{3} X_n\, v_n \cosh(k_n\, d/2) = 0 \quad (m_y = 0) \ . \tag{32'}$$

In Eqs. (29)–(32'), d is the thickness of the film and X_n is the field strength of $h_t(n)$. The rf field h_0 is the magnetic field at the surface and, like $h_t(n)$ and $m_t(n)$, is transverse to $\vec{M}_0$. For either set of boundary conditions, the equations can be written in the form

$$[B] \cdot \vec{Y} = 0 \ ,$$

where $[B]$ is a 4×4 matrix and the components of the vector $\vec{Y}$ are h_0, X_1, X_2, and X_3. For unpinned spins, the matrix $[B]$ is given by

$$[B] = \begin{bmatrix} 1 & \cosh(k_1\, d/2) & \cosh(k_2\, d/2) & \cosh(k_3 d/2) \\ Z & k_1 \sinh(k_1\, d/2) & k_2 \sinh(k_2\, d/2) & k_3 \sinh(k_3\, d/2) \\ 0 & k_1 Q_1 \sinh(k_1\, d/2) & k_2 Q_2 \sinh(k_2\, d/2) & k_3 Q_3 \sinh(k_3\, d/2) \\ 0 & k_1\, v_1 \sinh(k_1\, d/2) & k_2\, v_2 \sinh(k_2\, d/2) & k_3\, v_3 \sinh(k_3\, d/2) \end{bmatrix}$$

There exist nontrivial solutions for $\vec{Y}$, if

$$\det[B] = 0 \ .$$

After expanding the determinant, we obtain the surface impedance

$$Z = \rho/\Delta \ , \tag{33}$$

where

$$\rho = (Q_2 - Q_1)(v_3 - v_1) - (v_2 - v_1)(Q_3 - Q_1)$$

$$\Delta = \frac{Q_2 v_3 - v_2 Q_3}{k_1 \tanh(k_1\, d/2)} + \frac{Q_3 v_1 - v_3 Q_1}{k_2 \tanh(k_2\, d/2)} + \frac{Q_1 v_2 - v_1 Q_2}{k_3 \tanh(k_3\, d/2)} \ .$$

For full pinning, the surface impedance is

$$Z = \Delta'/\rho \ , \tag{34}$$

where

$$\Delta' = (Q_2 v_3 - v_2 Q_3)\, k_1 \tanh(k_1\, d/2) + (Q_3 v_1 - v_3 Q_1)\, k_2 \tanh(k_2\, d/2) + (Q_1 v_2 - v_1 Q_2)\, k_3 \tanh(k_3\, d/2) \ .$$

The power absorbed by the sample is given by[23]

$$P = \mathrm{Re}[Z] \ . \tag{35}$$

The resonance field is defined in the conventional way as the field ω/γ for which $dP/d(\omega/\gamma) = 0$. The linewidth is obtained from the peak-to-peak width of the derivative of the resonance line.

III. RESULTS

Ideally one would like to calculate the FMR-frequency field and linewidth as functions of K_1 and K_2 while the values of other parameters are fixed. However, this is unrealistic for any magnetic metal of interest. As an example, for nickel the values of K_1 and K_2 can be varied by either varying the temperature of the sample or alloying the sample with another element such as copper or palladium. However, as the temperature or the alloy composition is varied, the conductivity, the magnetization, the magnetic damping, and the g factor are also affected.

We describe here the results of calculations for Ni at two temperatures, 300 and 77 °K. The values of $4\pi M_0$, σ, K_1, K_2, λ, and g were obtained from published values.[5–8,24] Since σ is a structure-sensitive property, we have varied it over a reasonable range at each temperature. We expect a marked contrast between the results at the two temperatures since K_1, K_2, and σ change by an order of magnitude between the two temperatures. The other parameters are reasonably constant between the two temperatures, although the magnetization does vary slightly.

We fix the frequency $\omega_0/2\pi$ and the in-plane

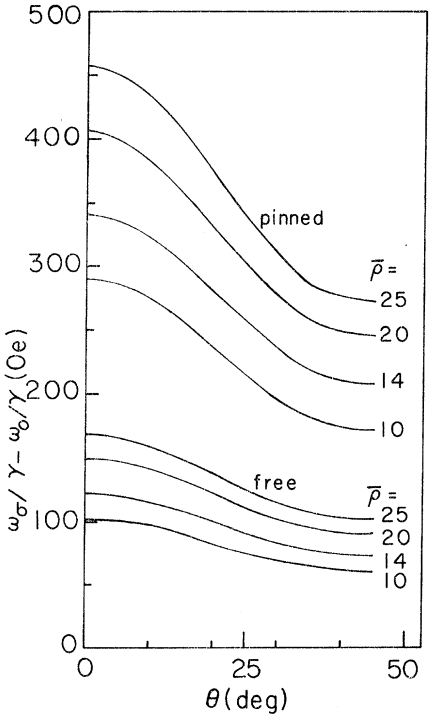

FIG. 2. Difference in resonant "effective" field between the field value obtained from metallic effects and the insulator value of 3072 Oe as a function of θ, the in-plane angle of $\vec{M}_0$. The angle θ is defined with respect to the $\langle 100 \rangle$ axis. The frequency is 9.44 GHz and the temperature is 77 °K. The resistivity ratio $\bar{\rho}$ is defined as the ratio of the resistance value at room temperature to resistance at 77 °K.

angle θ, and calculate the resonance static internal field $H_0(\theta)$, assuming an insulating medium. This is done by selecting a value of ω_0, and substituting it, along with appropriate values of K_1, K_2, M, and g, in Eq. (21) for a $\langle 001 \rangle$ direction, Eq. (22) for a $\langle 101 \rangle$ direction, or the appropriate simplification of Eq. (23) for arbitrary θ, to calculate $H_0(\theta)$. Then, for the appropriate θ, H_0 is kept fixed and the power absorbed by the sample per unit area is calculated as a function of frequency or of ω/γ using Eq. (35). The derivative of the absorption curve yields the shifted resonance frequency, the effective field ω_σ/γ, and the linewidth $\Delta\omega_\sigma/\gamma$ for a metal. In Table I we show the results for $\omega_0/2\pi = 9.44$ GHz, $\omega_0/\gamma = 3072$ Oe and for $\omega_0/2\pi = 24.0$ GHz, $\omega_0/\gamma = 7810$ Oe for a temperature of 300 °K. The resonance field shift for the unpinned case is the so-called exchange-conductivity shift.[2] For the pinned case, the shift is due to both exchange conductivity and pinning. We note that for either pinning condition both the shift and linewidth are approximately isotropic at both frequencies.

As the temperature is lowered, the values of $2K_1/M$, $2K_2/M$, and σ all increase. We would expect, therefore, that the resonance field shifts and linewidths would both increase and become more anisotropic. That this is the case is shown in Table II, for $T = 77$ °K. The low-temperature results are shown in greater detail in the series of figures. Figures 2 and 3 show resonance field shift as a function of θ for the two frequencies. The conductivity σ at 300 °K is given in Table I and results are shown for a variety of resistivity ratios $\bar{\rho}$. We note that there is a substantially greater anisotropy in the shift at the low frequency than there is at the high frequency. This is to be expected since $2K_1/M$ and $2K_2/M$ are a larger fraction of ω/γ or of H_0 at low frequency than at high frequency.

TABLE I. Room-temperature FMR field shift and linewidth.

f (GHz)	Direction of M_0	Resonance field shift $\omega_\sigma/\gamma - \omega_0/\gamma$ (Oe) Pinned	Unpinned	Linewidth $\Delta\omega_\sigma/\gamma$ (Oe) Pinned	Unpinned
9.44	$\langle 100 \rangle$	92	25	262	185
	$\langle 110 \rangle$	89	24	260	180
24.0	$\langle 100 \rangle$	94	20	448	323
	$\langle 110 \rangle$	92	19	444	321

$T = 300$ °K
$4\pi M = 6100$ G
$g = 2.19$
$\sigma = 1.42 \times 10^5$ mho/cm
$2K_1/M = -220$ Oe
$2K_2/M = -45$ Oe
$d = 1$ μm

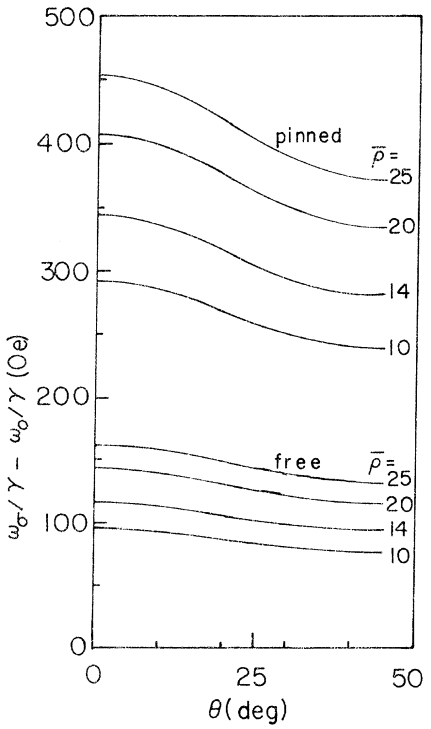

FIG. 3. Same as Fig. 2, except the frequency is 24 GHz.

TABLE II. Low-temperature FMR field shift and linewidth.

f (GHz)	Direction of M_0	Resonance field shift $\omega_0/\gamma-\omega_0/\gamma$ (Oe) Pinned	Unpinned	Linewidth $\Delta\omega_0/\gamma$ (Oe) Pinned	Unpinned
9.44	⟨100⟩	341	122	660	328
	⟨110⟩	207	73	424	216
24.0	⟨100⟩	343	116	806	460
	⟨110⟩	281	93	694	408

$T=77\,^\circ$K; $4\pi M=6350$ G; $g=2.19$; $\sigma=19.9\times10^5$ mho/cm; $2K_1/M=-3100$ Oe; $2K_2/M=-520$ Oe; $d=1$ μm

We note from Table I that linewidths at room temperature are nearly isotropic. From Table II, we see that they have become quite anisotropic at low temperature. This is again shown in greater detail in Figs. 4 and 5. However, part of the anisotropy at low temperature would be observed with an insulator. The size of this effect can be obtained either from the solution of Eq. (35) with the $\sigma=0$ version of Eq. (23) or from an approximate calculation, which works well for this case. First, for $\sigma=0$ we can put Eq. (23) into the form[25]

$$\left(\frac{\omega}{\gamma}\right)^2 - j\,\frac{\omega}{\gamma}\,\frac{\Delta\bar{\omega}}{\gamma} + \left(\frac{\omega_0}{\gamma}\right)^2 = 0\ ;$$

we have

$$\frac{\Delta\bar{\omega}}{\gamma} = \frac{2\lambda}{\gamma M}\left[H_0 + 2\pi M_0 - \tfrac{1}{2}(c_{11}+c_{22}+c_{33})\right], \tag{36}$$

where $\Delta\bar{\omega}/\gamma$ is the half-power point frequency field linewidth, if the line is Lorentzian. In this case the derivative linewidth $\Delta\omega_0/\gamma$ is obtained by multiplying $\Delta\bar{\omega}/\gamma$ by 0.577.[26] For $\vec{H}_0$ along the [001] axis, we use Eq. (21) and

$$\frac{\Delta\omega_0}{\gamma} \simeq 1.15\,\frac{\lambda}{\gamma M_0}\left(H_0 + 2\pi M + \frac{2K_1}{M_0}\right),$$

where H_0 is the internal field at *resonance* and is calculated from the resonance equations using either $\omega_0/\gamma=3072$ or 7810 Oe. For H_0 along the [101] axis, we use Eq. (22) and

$$\frac{\Delta\omega_0}{\gamma} \simeq 1.15\,\frac{\lambda}{\gamma M_0}\left(H_0 + 2\pi M_0 + \frac{K_1}{2M_0} + \frac{K_2}{4M_0}\right).$$

Putting appropriate values for $2\pi M_0 \simeq 3000$ G, $\lambda=3.75\times10^7$ Hz, and $\gamma=3.073\times10^6$ Hz/Oe, we obtain, at x band,

$$\Delta\omega_0/\gamma \simeq 121 \text{ Oe}, \quad \vec{H}_0 \parallel [001],$$

$$\Delta\omega_0/\gamma \simeq 105 \text{ Oe}, \quad \vec{H}_0 \parallel [101].$$

We see from the above that the insulator linewidth is $\frac{1}{2}$-$\frac{1}{5}$ of the total linewidth, depending on the pinning conditions. The rest of the linewidth is due to the metallic effect. Equation (36) accounts for only about $\frac{1}{9}$ of the anisotropy in the linewidth.

Finally, it should be pointed out that at low temperatures ($T\sim77\,^\circ$K) the skin depth begins to become anomalous in Ni. For lower temperatures, the effect of the exchange conductivity on the linewidth and field position is nearly constant. This means that if we were to "push" our calculations into the anomalous skin-depth temperature region, the curves (in Figs. 2–5) for different $\bar{\rho}$'s "approach" each other.

IV. DISCUSSION AND CONCLUSIONS

We have shown that for metals with large magnetocrystalline anisotropies and high conductivities

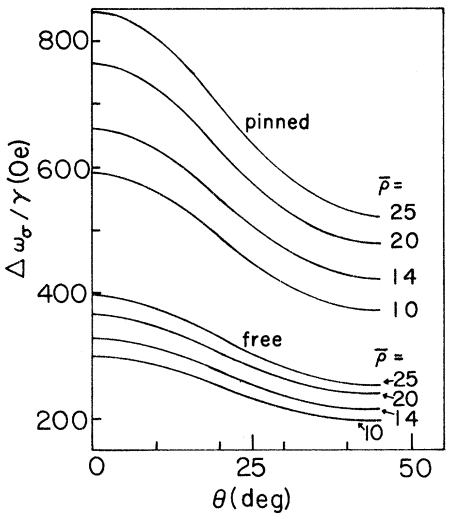

FIG. 4. FMR effective field linewidth as a function of θ, the in-plane angle of $\vec{M}_0$. The frequency is 9.44 GHz and the temperature is 77 °K. The resistivity ratio $\bar{\rho}$ is defined as in the caption of Fig. 2.

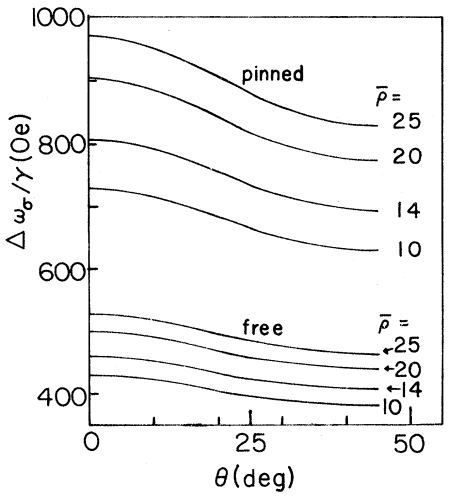

FIG. 5. Same as Fig. 4, except the frequency is 24 GHz.

there exist substantial anisotropies in the shift of resonance field from its insulator value and in the increase of resonance linewidth over its insulator value. While this result is intuitively reasonable, it has not previously been demonstrated. More important, the possibility of such an effect has usually been ignored in the analysis of FMR data for single-crystal metals. Ignoring the shift, in particular, can have very serious effects on an attempt to evaluate a consistent set of parameters appropriate to resonance experiments.

The procedure usually used in evaluating such data has been to assume an isotropic shift in resonant field due to the exchange-conductivity effect, and to fit the data with a resonance equation appropriate to an insulator. As we have shown, this is completely invalid for a material such as Ni at low temperatures. Let us use the results presented in Table II to illustrate the consequences of this procedure. For a sample whose properties have the values given in the table, with pinned surface spins, at 9.44 GHz, the difference in resonance field for the $\langle 100\rangle$ and $\langle 110\rangle$ directions in the film plane, over and above that which would be measured for an insulator, is $341 - 207 = 134$ Oe. If we were to attempt to interpret these data in terms of Eqs. (21) and (22), we would be obliged to use incorrect values for M_0, K_1, K_2, or γ. If we were to use the values of M_0, K_1, and K_2 known from other experiments, we would be obliged to interpret the results in terms of an anisotropy in γ or in the g factor. Thus,

$$134 = \omega_0 \left(\frac{1}{\gamma_{\langle 100\rangle}} - \frac{1}{\gamma_{\langle 110\rangle}} \right) .$$

Therefore, for the pinned case,

$$\frac{\Delta g}{g_{\langle 100\rangle}} = \frac{134}{\omega_0/\gamma_{\langle 100\rangle}} \simeq 0.045 .$$

For the unpinned case, $\Delta g/g_{\langle 100\rangle} \simeq 0.015$.

One of the approximate schemes[5,27] to incorporate exchange-conductivity resonance field shifts in an anisotropic medium has been to write H_a in Eqs. (21) and (22) as $H_a - \delta H_a$, where δH_a is a fictitious exchange-conductivity shift. Furthermore, δH_a was assumed isotropic, which is contrary to our findings. Using this approximation, Rodbell[5] and Frait and Gemperle[27] found at X band that the g factor was isotropic for nickel and iron, respectively.

However, substituting the FMR fields measured by Rodbell[5] in $\{100\}$ nickel platelets along the $\langle 100\rangle$ and $\langle 110\rangle$ axes and the values of $4\pi M_0$, K_1, and K_2 obtained for torque measurements[8] on spherical nickel samples into Eqs. (21) and (22), Aubert[8] deduced that the g factor was anisotropic ($\Delta g/g_{\langle 100\rangle} \simeq 0.08$) at X band and at a temperature of $\sim 130\,^{\circ}$K. We predict an anisotropic exchange shift which may be interpreted as an anisotropic g factor with a value of $\Delta g/g_{\langle 100\rangle} = 0.01$ to 0.04, depending on the boundary condition. The discrepancy between our estimate and that of Aubert may be due to the fact that the values of K_1, K_2, and possibly K_3 are frequency dependent. The values of K_1 and K_2 obtained by Rodbell[5] from FMR field measurements at *X band* were different from the values of these constants obtained by Aubert[8] at low frequency (audio frequency). An investigation of the frequency dependence of K_1 and K_2 is presently being carried out. Since there may be a number of effects which can account for the anisotropy in the g factor, it is crucial that a reasonable estimate be obtained for the anisotropic shift in the resonant field due to the exchange-conductivity effect.

Linewidth anisotropies such as we have discussed above have been observed experimentally and reported previously.[28,29] It should be noted, if one wishes to compare the theory described here with experiment, that the calculations here have been done, for convenience, in terms of frequency sweep. Experimental results are almost always reported in terms of field sweep. To compare the two it is necessary to convert applied field to effective field or vice versa.[7]

Note added in proof. The addition of a field of the form $(2k_1/M)(\alpha_1\vec{a}_x + \alpha_2\vec{a}_y + \alpha_3\vec{a}_z)$ to Eq. (4) does not modify either the equilibrium condition contained in Eq. (4) or the resulting secular equations, since this field always aligns along the internal field.

ACKNOWLEDGMENTS

The authors wish to thank Dr. G. T. Rado and Professor S. Bhagat for helpful discussions.

APPENDIX: DEFINITION OF SOME TERMS

The definition of each term in the matrix of $[A]$ is given below:

$$a_{11} = -\left[a(1-\alpha_1^2) + \Omega\right] ,$$

$$a_{12} = c\alpha_3 + d\alpha_1\alpha_2 ,$$

$$a_{13} = -b\alpha_2 + a\alpha_1\alpha_3 ,$$

$$a_{21} = -b\alpha_3 + a\alpha_1\alpha_2 ,$$

$$a_{22} = -\left[d(1-\alpha_2^2) + \Omega\right] ,$$

$$a_{23} = b\alpha_1 + a\alpha_2\alpha_3 ,$$

$$a_{31} = b\alpha_2 + a\alpha_1\alpha_3 ,$$

$$a_{32} = -c\alpha_1 + d\alpha_2\alpha_3 ,$$

$$a_{33} = -\left[a(1-\alpha_3^2) + \Omega\right] ,$$

where

$$\Omega = j\omega/\gamma ,$$

$$a = \frac{\lambda}{\gamma}\left(\frac{H_0}{M_0} + \frac{1}{Q}\right),$$

$$b = H_0 + \frac{M_0}{Q} - \frac{2A}{M_0}k^2,$$

$$c = H_0 + 4\pi M_0 - \frac{2A}{M_0}k^2,$$

and

$$d = \frac{\lambda}{\gamma}\left(\frac{H_0}{M_0} + 4\pi\right),$$

$$c_{11} = b_{11} + \frac{\lambda}{\gamma M_0}(A\alpha_1 - C_1),$$

$$c_{12} = b_{12} + \frac{\lambda}{\gamma M_0}(B\alpha_1 - C_2),$$

$$c_{13} = b_{13} + \frac{\lambda}{\gamma M_0}(C\alpha_1 - C_3),$$

$$c_{21} = b_{21} + \frac{\lambda}{\gamma M_0}(A\alpha_2 - C_4),$$

$$c_{22} = b_{22} + \frac{\lambda}{\gamma M_0}(B\alpha_2 - C_5),$$

$$c_{23} = b_{23} + \frac{\lambda}{\gamma M_0}(C\alpha_2 - C_6),$$

$$c_{31} = b_{31} + \frac{\lambda}{\gamma M_0}(A\alpha_3 - C_7),$$

$$c_{32} = b_{32} + \frac{\lambda}{\gamma M_0}(B\alpha_3 - C_8),$$

$$c_{33} = b_{33} + \frac{\lambda}{\gamma M_0}(C\alpha_3 - C_9),$$

where

$$A = \alpha_1\left(6\frac{K_1}{M_0}(1-\alpha_1^2) + 10\frac{K_2}{M_0}\alpha_2^2\alpha_3^2\right),$$

$$B = \alpha_2\left(6\frac{K_1}{M_0}(1-\alpha_2^2) + 10\frac{K_2}{M_0}\alpha_1^2\alpha_3^2\right),$$

$$C = \alpha_3\left(6\frac{K_1}{M_0}(1-\alpha_3^2) + 10\frac{K_2}{M_0}\alpha_1^2\alpha_2^2\right),$$

and, finally,

$$b_{11} = \frac{4K_2}{M_0}\alpha_1\alpha_2\alpha_3(\alpha_3^2 - \alpha_2^2),$$

$$b_{12} = -b_{32} = \frac{2K_1}{M_0}\alpha_3(1-3\alpha_2^2) + \frac{2K_2}{M_0}\alpha_3\alpha_1^2(\alpha_3^2 - 2\alpha_2^2),$$

$$b_{13} = -b_{23} = \frac{2K_1}{M_0}\alpha_2(3\alpha_3^2 - 1) + \frac{2K_2}{M_0}\alpha_2\alpha_1^2(2\alpha_3^2 - \alpha_2^2),$$

$$b_{21} = -b_{31} = \frac{2K_1}{M_0}\alpha_3(3\alpha_1^2 - 1) + \frac{2K_2}{M_0}\alpha_3\alpha_2^2(2\alpha_1^2 - \alpha_3^2),$$

$$b_{22} = \frac{4K_2}{M_0}\alpha_1\alpha_2\alpha_3(\alpha_1^2 - \alpha_3^2),$$

$$b_{33} = \frac{4K_2}{M_0}\alpha_1\alpha_2\alpha_3(\alpha_2^2 - \alpha_1^2).$$

*Supported in part by the National Science Foundation under Grant No. GH-33006.

[1]E. Cech, Acta Metall. **9,** 459 (1961); R. W. DeBlois, J. Appl. Phys. **36,** 1948 (1965).
[2]W. S. Ament and G. T. Rado, Phys. Rev. **97,** 1558 (1955).
[3]A. I. Akhiezer *et al.,* Usp. Fiz. Nauk **72,** 3 (1960) [Sov. Phys.-Usp. **3,** 661 (1961)].
[4]C. Vittoria, R. C. Barker, and A. Yelon, J. Appl. Phys. **40,** 1561 (1969).
[5]D. S. Rodbell, Physics **1,** 279 (1965); H. Nosé, J. Phys. Soc. Jap. **15,** 1714 (1960).
[6]S. M. Bhagat and L. L. Hirst, Phys. Rev. **151,** 401 (1966).
[7]C. Vittoria, R. C. Barker, and A. Yelon, Phys. Rev. Lett. **19,** 792 (1967).
[8]G. Aubert, C.R. Acad. Sci. (Paris) **260,** 3313 (1965); G. Aubert, thesis (Grenoble University, 1968) (unpublished).
[9]C. Vittoria and G. C. Bailey, Phys. Status Solidi (a) **9,** 283 (1972).
[10]G. C. Bailey and C. Vittoria, Phys. Rev. Lett. **28,** 100 (1972).
[11]S. M. Bhagat and M. S. Rothstein, J.Phys.(Paris) **32,** 777 (1971).
[12]P. W. Anderson and M. T. Weiss, Phys. Rev. **98,** 925 (1955).
[13]J. R. Anderson, S. M. Bhagat, and F. L. Cheng, Phys. Status Solidi (b) **45,** 357 (1971).
[14]Z. Frait, L. Pauling-Tothova, and M. Vesela, Czech. J. Phys. **20,** 1268 (1970).
[15]G. T. Rado and J. R. Weertman, J. Phys. Chem. Solids **11,** 315 (1959).
[16]T. G. Phillips. L. W. Rupp, R. C. Barker, A. Yelon, and C. Vittoria, J. Phys. (Paris) **32,** 1162 (1971).
[17]C. Vittoria and G. C. Bailey, Solid State Commun. **9,** 1271 (1971).
[18]R. W. Damon and J. R. Eschbach, J. Phys. Chem. Solids **19,** 308 (1961).
[19]B. Lax and K. J. Button, *Microwave Ferrites and Ferrimagnetics* (McGraw-Hill, New York, 1962).
[20]J. Smit and H. P. J. Wijn, Philips Res. Rep. **10,** 113 (1955).
[21]*Handbook of Mathematical Functions,* edited by M. Abramowitz and I. A. Stegun (Dover, New York, 1965), p. 17.
[22]A. I. Akhiezer, V. G. Bar'yakhtar, and S. V. Peletminskii, *Spin Waves* (North-Holland, New York, 1968), p. 105.
[23]In Ref. 10, P should have been written $P = \mathrm{Re}[Z^{(o)}|h_o|^2 + Z^{(d)}|h_d|^2]$ instead of $P = Z^{(o)}|h_o|^2 + Z^{(d)}|h_d|^2$.
[24]*American Institute of Physics Handbook* (McGraw-Hill, New York, 1963).
[25]G. V. Skrotskii and L. V. Kurbatov, Zh. Eksp. Teor. Fiz. **35,** 216 (1958) [Sov. Phys.-JETP 38, 148 (1959)].
[26]C. Poole, *E. S. R. Spin Resonance* (Interscience, New York, 1967).
[27]Z. Frait and R. Gemperle, J. Phys. (Paris) **32,** 541 (1971).
[28]T. D. Rossing and R. Bjork, J. Appl. Phys. **38,** 4920 (1967).
[29]W. Anders, D. Bastian, and L. Biller, Z. Angew. Phys. **32,** 12 (1971).